

NLO corrections merged with parton showers for $Z + 2$ jets production using the POWHEG method

Emanuele Re

*Institute for Particle Physics Phenomenology, Department of Physics
University of Durham, Durham, DH1 3LE, UK*

E-mail: emanuele.re@durham.ac.uk

ABSTRACT: We present results for the QCD production of $Z/\gamma + 2$ jets matched with parton showers using the POWHEG method. Some technicalities relevant for the merging of NLO corrections for this process with parton showers are discussed, and results for typical distributions are shown, in presence of different sets of cuts. A comparison with ATLAS data is also presented, and good agreement is found.

KEYWORDS: QCD Phenomenology, NLO Computations, Jets, Hadronic Colliders, Monte Carlo Simulations

Contents

1	Introduction	1
2	Method and details of the implementation	2
3	Results	4
3.1	Comparison with NLO predictions	4
3.2	Comparison with LHC data	8
4	Conclusions	9
A	One-loop virtual amplitudes	10

1 Introduction

The process of vector boson production in association with jets is a very important Standard Model process at hadron colliders. W -boson production in association with jets is a typical background for many new-Physics searches, and it is also interesting as a process in itself to study jets at hadron colliders. The production of a Z -boson in association with jets present similar features, since for example when the Z decays in a neutrino pair one can have a “missing energy + jets” signature [1], and it is also a reducible background for ZH production, similarly to the $W + 2$ jets case for WH production. Moreover, the production of a Z -boson in association with 2 jets is also one of the backgrounds to Higgs-boson production via vector-boson fusion (VBF), for example when the Higgs decays in a $\tau^+\tau^-$ pair. In particular, the signal-background separation between Hjj via VBF and Zjj relies on the very different kinematical properties of the jets produced in association with the heavy boson [2, 3].

For the above reasons, it is important to reach a high-level of accuracy in the predictions for the production of $Z + 2$ jets at hadron colliders. The full Next-to-Leading Order (NLO) corrections for this process have been computed in refs. [4, 5] for the QCD production, and in ref. [6] for the electroweak production. Nowadays, one of the methods to improve upon existing NLO computations is to merge them with parton showers. This has been realized with the MC@NLO [7, 8] and the POWHEG [9, 10] methods for a number of processes of increasing complexity [11–16]. In particular, in the recent past, $W + 2$ and $W + 3$ jets have been implemented with the MC@NLO method [17, 18], and $H + 2$ jets using POWHEG [19]. Given the role played by jet activity in many searches where $Z + 2$ jets is a background, it is important to achieve the same level of accuracy for this process as well.

In this paper NLO corrections for the QCD production of $Z/\gamma + 2$ jets merged with parton showers according to the POWHEG method are presented for the first time. Effects

due to photon exchange and all the spin correlations of the decay products of the Z/γ intermediate state have been fully taken into account in the implementation, although in the following we will refer to the process simply as “ $Z + 2$ jets production”. We will concentrate here mainly on the implementation procedure and on the discussion of the results we obtained, in presence of different cuts, leaving a broader phenomenological study for future work, although a comparison with the first available LHC data is presented.

2 Method and details of the implementation

To simulate with NLO matched with parton shower (NLO+PS) accuracy the $Z + 2$ jets process, the POWHEG BOX package [20] has been used. The POWHEG BOX is a program that automates all the steps described in ref. [10], turning a NLO calculation into a POWHEG simulation. The details of how the program works have been largely described in ref. [20], and therefore will not be repeated in this paper. In this section, we first summarize how the inputs needed by the package to work were obtained, and we then describe some technical details relevant for this implementation.

The Born matrix elements have been computed using the helicity-amplitude technique of refs. [21, 22]. By keeping the amplitude uncontracted with respect to the gluon polarization vector, the spin-correlated Born matrix elements ($\mathcal{B}_{\mu\nu}$, defined in eq. (2.8) of ref. [10]) are easily obtained. The color-connected squared amplitudes (\mathcal{B}_{ij} , defined in eq. (2.97) of ref. [10]) for this process are not proportional to the Born squared amplitudes. They have been computed inserting the color factors correspondent to the product of two color operators $\mathbf{T}_i \cdot \mathbf{T}_j$ while computing the terms needed to build the Born squared matrix elements.¹ Real corrections have been obtained using MadGraph4 [23], whereas the virtual corrections, first computed in ref. [24], have been obtained linking the POWHEG BOX with BlackHat [25], using the interface proposed in ref. [26]. A sample of Feynman diagrams that enter the Born and the virtual contributions is reported in fig. 1, whereas some numerical values for the finite part of the virtual corrections are reported in Appendix A.

Several checks have been performed at this stage: spin-correlated and color-linked squared amplitudes have been checked numerically, by comparing the soft and collinear limits of the real matrix elements with the expected value obtained from the factorization formulas for collinear and soft emissions, respectively. Thanks to the aforementioned interface, BlackHat also returns the coefficients of the double and the single pole of the one-loop corrections: this allows for an extra cross check of the color-linked amplitudes, or, viceversa, a check that the interface for the 2 codes is working properly. As a final important check, several distributions have also been compared against NLO predictions obtained from n-tuples generated with BlackHat+SHERPA [27, 28], and agreement has been found.

¹Similarly, the relative weights of each colour structure present in the Born processes, in the limit of large number of colours, have been computed combining the terms needed to build the Born matrix elements. These weights are used to probabilistically assign a planar colour structure to the underlying-Born kinematics, from which a color flow is attached to the generated events, using the prescription described in refs. [10, 20].

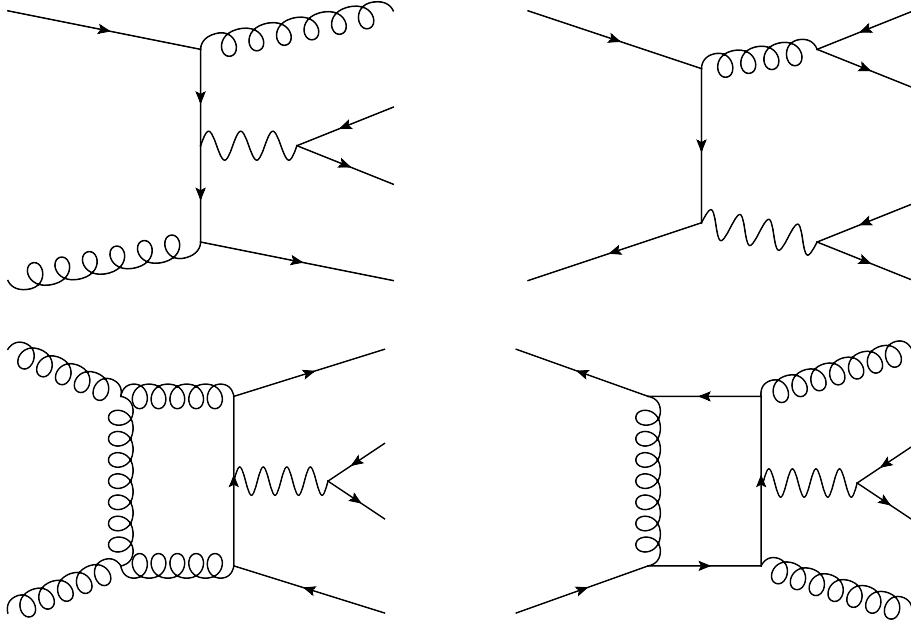


Figure 1. Sample graphs for the Born and the virtual contributions to the $Z/\gamma + 2$ jets production process.

The significant property of a process like $V + 2$ jets, that makes it more difficult to implement than $V + 1$ jet, is the fact that the Born matrix elements are singular in several regions. In order to suppress the singularities of the underlying-Born amplitudes, instead of using sharp generation cuts, we used a suppression factor that vanishes when at least one of these regions is approached. As explained in [11], this means that the underlying-Born kinematics is generated according to a modified \bar{B} function

$$\bar{B}_{\text{supp}}(\Phi_n) = \bar{B}(\Phi_n) F(\Phi_n), \quad (2.1)$$

where \bar{B} is the inclusive NLO cross section at fixed underlying-Born variables, and, for the case at hand, we used

$$F(\Phi_n) = \left(\frac{p_{T,1}^2}{p_{T,1}^2 + \Lambda_{p_T}^2} \right)^{k_{\text{IS}}} \left(\frac{p_{T,2}^2}{p_{T,2}^2 + \Lambda_{p_T}^2} \right)^{k_{\text{IS}}} \left(\frac{s_{1,2}}{s_{1,2} + \Lambda_m^2} \right)^{k_{\text{FS}}}. \quad (2.2)$$

Φ_n is the Born phase space, $p_{T,1}$ and $p_{T,2}$ are the transverse momenta of the 2 outgoing light partons in the underlying-Born kinematics and $s_{1,2}$ is the invariant mass squared obtained from their momenta. Since the Born-like kinematics, from which the radiation is generated, is distributed according to eq. (2.1), the generated events will be assigned a weight proportional to $1/F$. To obtain the results shown in the next section, we have set $k_{\text{IS}} = k_{\text{FS}} = 2$, $\Lambda_{p_T} = 10$ GeV and $\Lambda_m = 5$ GeV. We also notice here that a similar method has been recently used in ref. [19] to implement in POWHEG the $H + 2$ jets process.

3 Results

3.1 Comparison with NLO predictions

In this section we present results obtained after showering and hadronizing the partonic events generated with POWHEG. We have used PYTHIA 6.4.25 with the ‘‘Perugia 0’’ tune enabled. We have considered $Z(\rightarrow e^+e^-) + 2$ jets production at the LHC, with an hadronic center-of-mass energy $\sqrt{S} = 7$ TeV.

The values of physical parameters entering the computation are the following:

$$m_Z = 91.1876 \text{ GeV}, \quad \Gamma_Z = 2.49 \text{ GeV}, \quad \alpha_{\text{em}}^{-1} = 128.802, \quad \sin^2 \theta_W = 0.23, \quad (3.1)$$

and we have used the CTEQ6M [29] parton distribution functions. In the computation of the \bar{B} function, the renormalization and factorization scales have been chosen equal to $\hat{H}_T/2$, where

$$\hat{H}_T = \sqrt{m_Z^2 + p_{T,Z}^2} + p_{T,1} + p_{T,2}, \quad (3.2)$$

$p_{T,Z}$ is the transverse momentum of the Z -boson, and all the quantities are computed using the underlying-Born kinematics.

As far as technical parameters or special options of the POWHEG BOX program are concerned, we have kept them equal to their default value, and we have not used any folding in the integration of the radiation variables [11, 20]. In so doing, the fraction of negative-weight events amounts to be 21%. These events were kept in the final sample used for the analysis, although of course not all of them will contribute to the plots, since some will not pass the cuts.

Jets have been defined according to the anti- k_T algorithm [30–32], setting $R = 0.4$, and the following cuts have been enforced in the analysis:

$$\begin{aligned} 66.328 \text{ GeV} < m_{e^+e^-} < 116.048 \text{ GeV}, \quad p_{T,e} > 20 \text{ GeV}, \quad |y_e| < 2.5, \\ p_{T,j} > 30 \text{ GeV}, \quad |\eta_j| < 4.4. \end{aligned} \quad (3.3)$$

Events are accepted only if there are at least 2 jets passing the above cuts. We also remind that we have not used isolation cuts for the leptons, and that photon radiation off leptons have been switched off in the shower,² in order to allow for a clear comparison with the fixed order result.

In fig. 2 we show the transverse momentum spectra of the reconstructed Z boson ($p_{T,Z}$), of the positron (p_{T,e^+}), and of the hardest and second-hardest jet (p_{T,j_1}, p_{T,j_2}), whereas in fig. 3 the invariant mass of the system made by the 2 hardest jets (m_{jj}) and their azimuthal separation ($\Delta\Phi_{jj}$) is shown.

The agreement between the NLO predictions and the results after the shower and the hadronization stage is very good for these inclusive observables. Shapes are essentially unmodified, and very small differences can be observed in the lower panel of each plot, where the ratio between the showered result and the NLO is plotted.³ We have checked

²Photon radiation has been switched off by setting MSTJ(41)=3 in PYTHIA.

³Errors in the lower panels of all the plots in this article represent the error on the ratio between two results, obtained propagating the errors of each set.

that they are of the same order of the theoretical uncertainty of the NLO result, obtained by changing the renormalization and factorization scales by the usual factors $\{1/2, 2\}$. It is also worth noticing that effects of the same order have been observed in other NLO+PS implementations of similar complexity [17, 18], although in presence of different cuts.

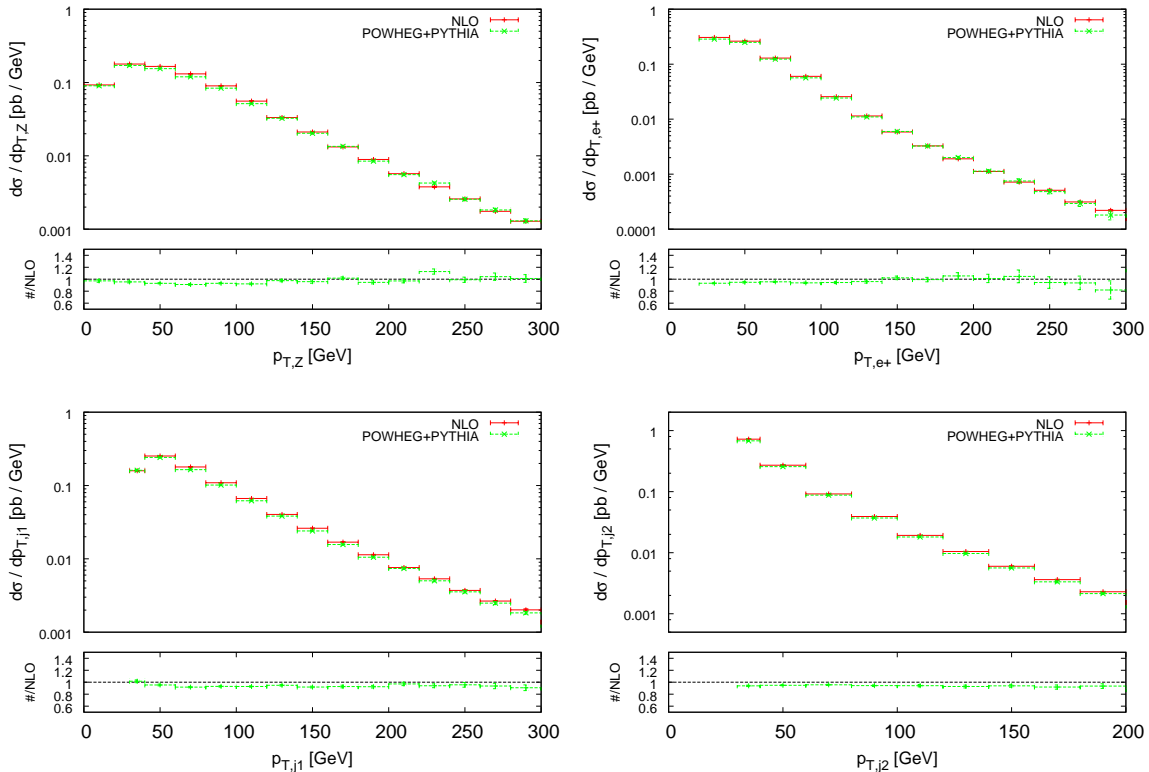


Figure 2. Comparisons between POWHEG (interfaced to PYTHIA) and the NLO results at the LHC pp collider ($\sqrt{S} = 7$ TeV), for the transverse momenta of the reconstructed Z -boson, of the positron (upper panel), of the hardest and of the second-hardest jet (lower panel). Vertical bars correspond to statistical errors.

In the upper panel of fig. 4 we show instead the transverse momentum of the third hardest jet and $H_{T,j}$, which is defined to be the scalar sum of all the jets transverse momenta: good agreement is found between the NLO result and the POWHEG+PYTHIA prediction for these observables as well. In particular, for values of p_{T,j_3} far from the low p_T region, the results after the showering and hadronization stage agree with the fixed order result (which has leading-order accuracy for this observable). In the small transverse momentum region, the NLO+PS prediction for p_{T,j_3} is expected to show Sudakov damping, as opposite to the NLO result, which diverges: this is noticeable in the lower panel of fig. 4, where we plot p_{T,j_3} removing the lower cut on the transverse momentum of all but the two hardest jets. The results obtained just after the parton-shower stage performed by PYTHIA are also shown for this observable. Sudakov damping is clearly present in all the curves where resummation of soft-collinear emissions is performed, although in the very low- p_T

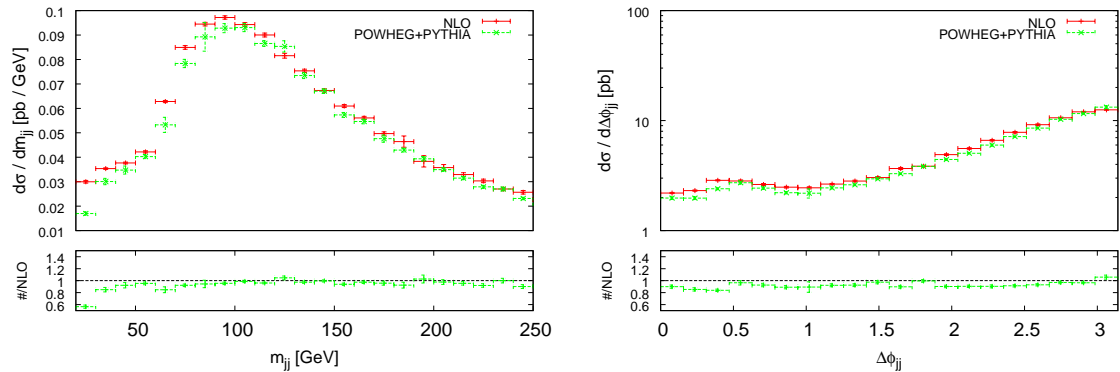


Figure 3. Comparisons between POWHEG (interfaced to PYTHIA) and the NLO results at the LHC pp collider ($\sqrt{S} = 7$ TeV), for the invariant mass of the two hardest jets and for their azimuthal separation. Vertical bars correspond to statistical errors.

region non-perturbative effects seem to play a small but noticeable role.

We have also performed the same analysis using as factorization and renormalization scale the Z -boson transverse mass, computed with the underlying-Born kinematics ($\mu = E_{T,Z} = \sqrt{m_Z^2 + p_{T,Z}^2}$), and we have found similar results.

As mentioned in the introduction, Zjj production is a background for Higgs-boson production via VBF, when the $H \rightarrow \tau\tau$ decay channel is considered in the analysis. For this reason it is interesting to check how typical distributions look like for the QCD Zjj background, in presence of a minimal set of VBF cuts. We chose

$$\begin{aligned}
 p_{T,\ell} &> 20 \text{ GeV}, & |y_\ell| &< 2.5, \\
 |\eta_j| &< 5.0, & p_{T,j} &> 20 \text{ GeV}, & p_{T,j_{\text{tag}}} &> 30 \text{ GeV}, \\
 |\eta_{j_1} - \eta_{j_2}| &> 4.0, & \eta_{j_1} \cdot \eta_{j_2} &< 0, \\
 \min(\eta_{j_1}, \eta_{j_2}) + 0.4 &< \eta_{\ell^+/\ell^-} &< \max(\eta_{j_1}, \eta_{j_2}) - 0.4,
 \end{aligned} \tag{3.4}$$

and we restricted the invariant mass of the lepton pair to lie in the interval $[66.328, 116.048]$ GeV.

The “tagging jets” are the two hardest jets, and we have used as before the anti- k_T algorithm, with $R = 0.4$. For this analysis we have generated the events using as factorization and renormalization scale the Z -boson transverse mass, computed with the underlying-Born kinematics. Moreover, multiple parton interactions have been switched off.

In the upper panel of fig. 5 we show $p_{T,Z}$ and p_{T,j_1} , whereas in the lower panel we show the azimuthal decorrelation between the two hardest jets and the shifted rapidity $y^{\text{rel}} = y_{j_3} - (y_{j_1} + y_{j_2})/2$, which is an useful quantity to measure the distance between the tagging jets and the third hardest jet.

Since we are using cuts designed to suppress the Zjj background, the statistical significance of the plots in fig. 5 is not optimal. However, we found that the results are not

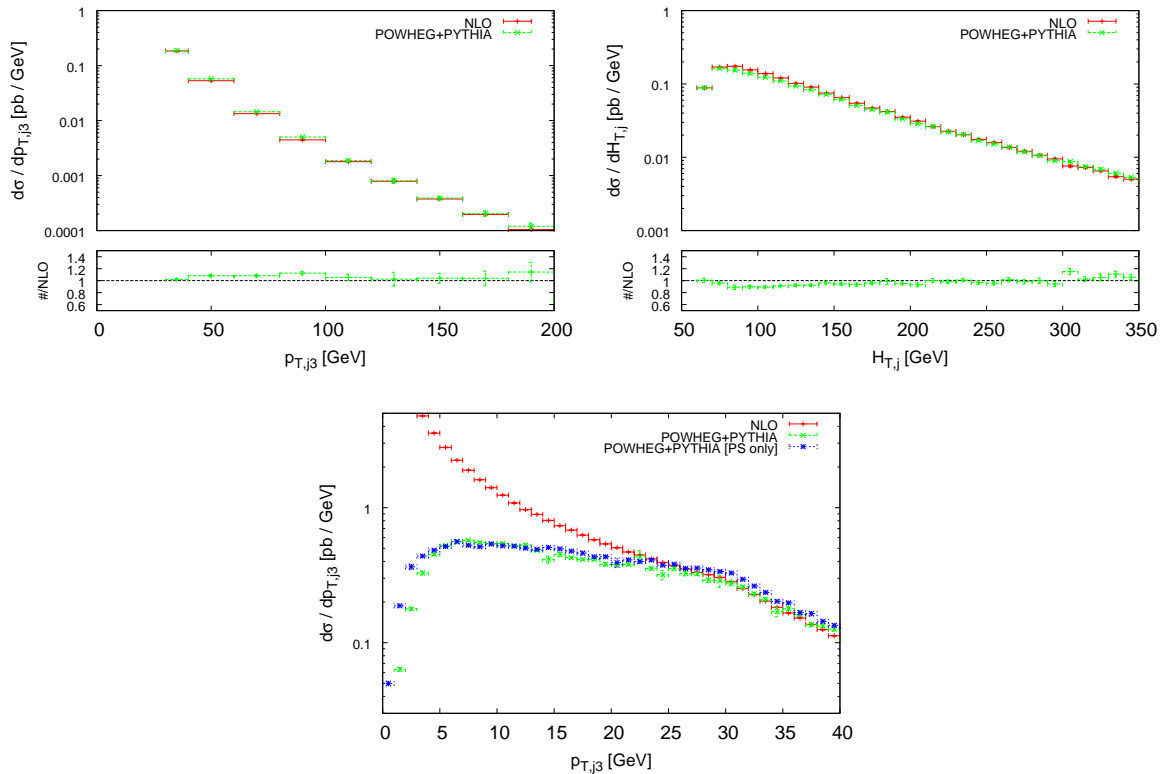


Figure 4. Comparisons between POWHEG (interfaced to PYTHIA) and the NLO results at the LHC pp collider ($\sqrt{S} = 7$ TeV), for the third hardest jets transverse momentum and for $H_{T,j}$ (upper panel). In the lower panel the low cut on the jets transverse momenta is kept only for the hardest and second-hardest jet. Vertical bars correspond to statistical errors.

changed sizeably when going from a NLO to a NLO+PS prediction. In particular y^{rel} is peaked at 0, whereas, as a consequence of the VBF cuts, the rapidity of the two tagging jets (not shown) is peaked at $|y_{j_{\text{tag}}}| \simeq 2.5$. This is the expected behaviour, since the QCD production of Zjj is a process dominated by quark or gluon exchange in the t -channel, and therefore one expects to observe a third jet in the central rapidity region, as opposite to what happens in processes dominated by a t -channel exchange of a colourless state, like Higgs-boson production via VBF or Zjj EW production. In the latter cases, the extra jet activity tends to be close to one of the two tagging jets, and, as a consequence, y^{rel} peaks at high rapidities and exhibits a dip at $y^{\text{rel}} = 0$ [33, 34]. The azimuthal decorrelation between the tagging jets is also particularly relevant: indeed it was shown that properties of the Higgs-boson such as its parity could be measured when it is produced via VBF, by looking at the azimuthal separation between the tagging jets [35]. This distribution appears to be stable as well for the Zjj background, when going from NLO to NLO+PS accuracy.

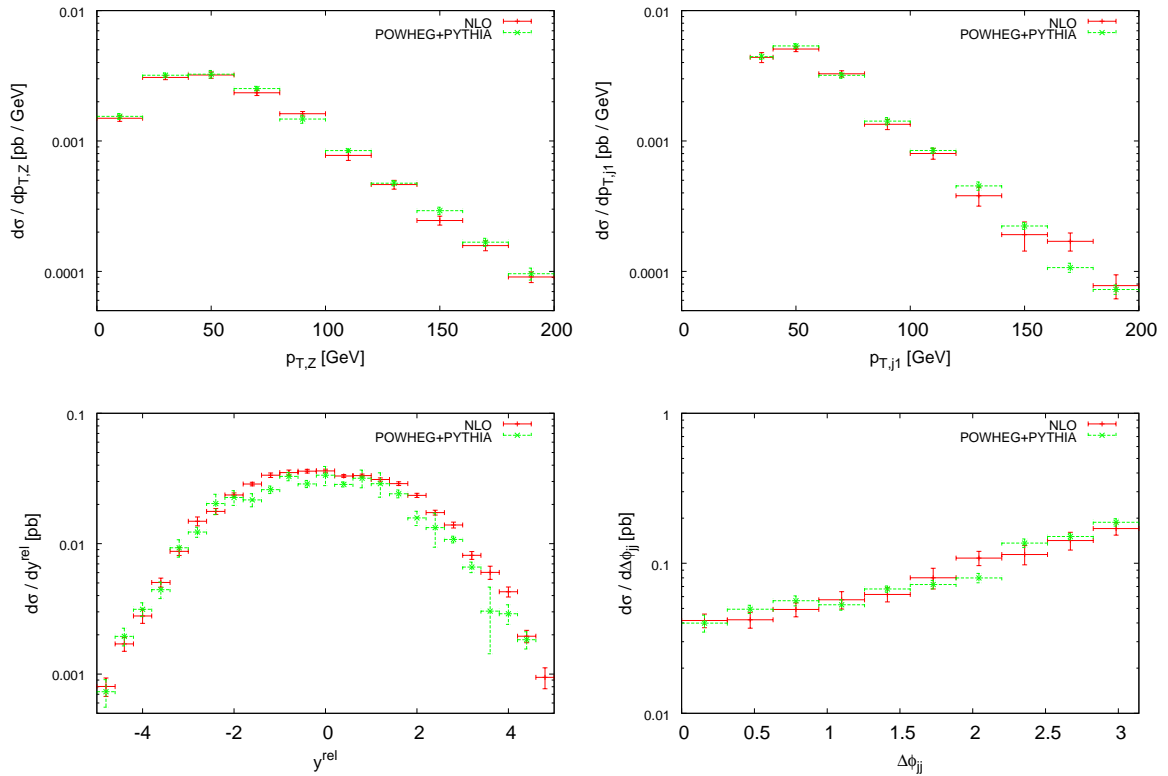


Figure 5. Comparisons between POWHEG (interfaced to PYTHIA) and the NLO results at the LHC pp collider ($\sqrt{S} = 7$ TeV) in presence of the VBF cuts of eq. (3.4): in the upper panel the transverse momenta of the reconstructed Z -boson and of the hardest jet are shown, whereas in the lower panel the azimuthal decorrelation between the tagging jets and $y^{\text{rel}} = y_{j_3} - (y_{j_1} + y_{j_2})/2$ are reported. Vertical bars correspond to statistical errors.

3.2 Comparison with LHC data

The ATLAS Collaboration has published a study on the production of a Z -boson in association with jets [36], and good agreement has been found when comparing the experimental results with QCD NLO perturbative predictions and predictions from Monte Carlo generators implementing LO matrix elements matched with parton showers. In this section we show a comparison of our NLO+PS predictions with ATLAS data. The set of cuts we used is very similar to that of eq. (3.3). Here we ask for

$$\begin{aligned}
 66 \text{ GeV} &< m_{e^+e^-} < 116 \text{ GeV}, \\
 p_{T,e} &> 20 \text{ GeV}, \quad |y_e| < 2.5, \quad \Delta R_{j,e} > 0.5, \\
 p_{T,j} &> 30 \text{ GeV}, \quad |y_j| < 4.4,
 \end{aligned}
 \tag{3.5}$$

and jets are built with the anti- k_T algorithm, with $R = 0.4$.

In fig. 6 we show our predictions, obtained with the sample generated with $\mu = \hat{H}_T/2$, together with the ATLAS data. In the upper panel we show the transverse momentum of

the second-hardest jet and the invariant mass of the two hardest jets, for events with at least 2 jets. In the lower panel instead, the azimuthal separation $\Delta\Phi_{jj}$ between the two hardest jets and their distance $\Delta R_{jj} = \sqrt{(\Phi_{j_1} - \Phi_{j_2})^2 + (y_{j_1} - y_{j_2})^2}$ in the $\phi - y$ plane is reported. The outcome of these comparisons is that the agreement between experimental data and the POWHEG results is very good.

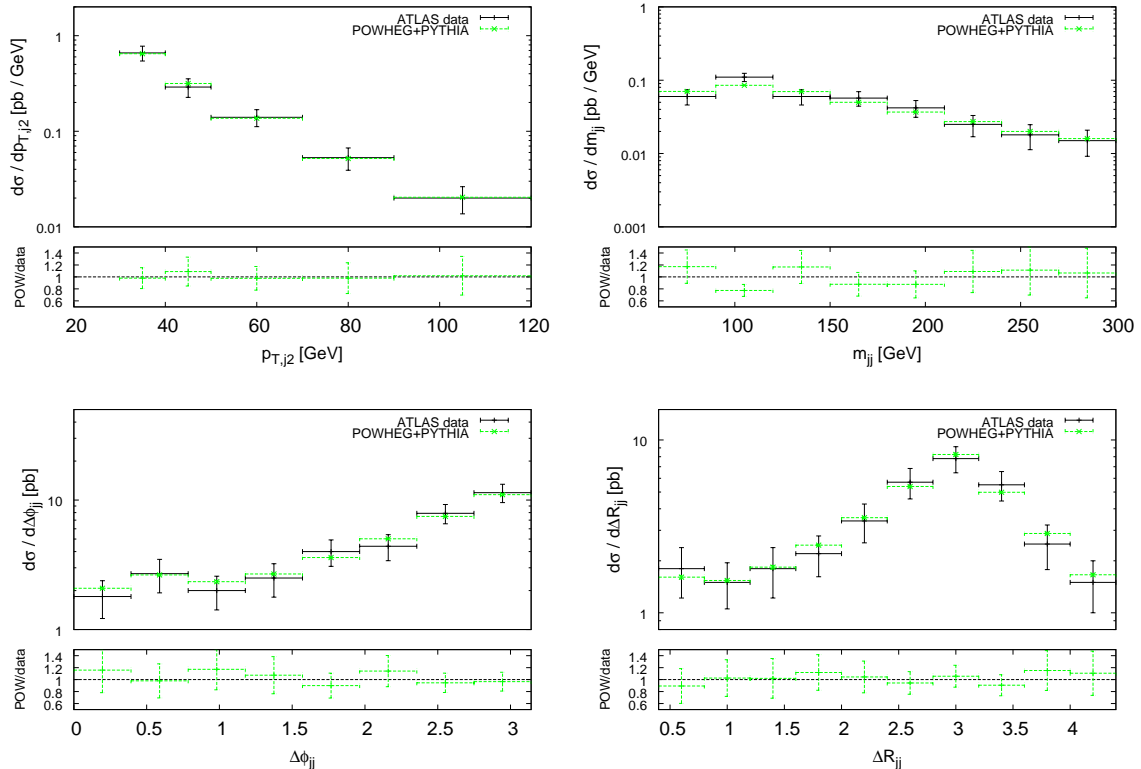


Figure 6. Comparisons between POWHEG (interfaced to PYTHIA) and the ATLAS data ($\sqrt{s} = 7$ TeV), in presence of the cuts of eq. (3.5), for the transverse momentum of the second-hardest jet, the invariant mass of the two hardest jets (upper panel), the azimuthal separation and the ΔR distance between the two hardest jets (lower panel). Vertical bars on the POWHEG results correspond to statistical errors, whereas bars on ATLAS data represent the sum (in quadrature) of the statistical and systematical errors reported in ref. [36].

4 Conclusions

In this paper we have described the first implementation of $Z + 2$ jets production at next-to-leading order in QCD, in the POWHEG framework. We have used the POWHEG BOX package, which is a program that automates the algorithm first proposed in ref. [9] and then described in detail in ref. [10]. The main purpose of this paper was to show that no particular problems occur in the implementation of complicated processes with POWHEG. This has been recently observed in ref. [19], and we obtained similar findings. We regulated

the divergent underlying-Born process by using a damped \bar{B} function, and we have shown that results are in good agreement with the fixed order for observables where they are expected to. Sudakov damping is instead present for observables sensitive to multiple soft-collinear emissions, such as the low- p_T region of the transverse momentum of the third hardest jet.

An important phenomenological application which can be performed having this processes available with NLO+PS accuracy is a study of the QCD radiation patterns of Zjj with respect to those present in Hjj production, especially in presence of cuts used in VBF searches. We have given an example of such a study by checking that typical observables in Zjj production in presence of VBF cuts have the behaviour expected from general properties of QCD, and they are not affected sizeably when going from NLO to a NLO+PS description. Further studies along these lines could also be performed using NLO+PS implementations of Hjj via gluon [19] and vector-boson fusion [34, 37] and $t\bar{t}$ (+ jets) [13, 14, 38], together with the Zjj implementation presented here.

Moreover, it could also be interesting to merge NLO+PS predictions for $Z + 2$ jets together with the same predictions for lower multiplicities, using for example the approach proposed in ref. [39]. These studies are left for future work.

We have also compared our NLO+PS results with recent ATLAS data, and we have found good agreement.

The computer code for this POWHEG implementation will soon be available within the public branch of the POWHEG BOX package. It will be possible to link it with public one-loop codes to evaluate the virtual corrections.

Acknowledgments

I would like to thank D. Maître for providing me with a version of the `BlackHat` code, and for very useful informatic help.

A One-loop virtual amplitudes

In this appendix, we report the numerical values of the finite part of virtual corrections for the following phase space point:

$$\begin{aligned}
p_{\oplus} &= (138.4784456174; 0.0000000000, 0.0000000000, 138.4784456174) \text{ GeV}, \\
p_{\ominus} &= (138.4784456174; 0.0000000000, 0.0000000000, -138.4784456174) \text{ GeV}, \\
p_{e^-} &= (39.8695145736; -30.2118421708, 7.3821554172, -24.9464740270) \text{ GeV}, \\
p_{e^+} &= (61.7949044527; 60.7995170788, -7.3821554172, -8.2178294395) \text{ GeV}, \\
p_1 &= (104.9831601822; -38.2721470356, 44.5354030781, 87.0247353101) \text{ GeV}, \\
p_2 &= (70.3093120261; 7.6844721276, -44.5354030781, -53.8604318436) \text{ GeV}.
\end{aligned}
\tag{A.1}$$

The finite parts of the interference between the tree-level and the one-loop amplitude (as returned by `BlackHat`), computed in the 't Hooft-Veltman scheme and stripped off of

subprocess	$ \mathcal{A}^{\text{tree}} ^2$	$2 \Re\{(\mathcal{A}^{\text{tree}})^* \cdot \mathcal{A}^{1\text{-loop}}\}$
$u\bar{u} \rightarrow e^- e^+ gg$	1.0489864146 E-005	1.7673954550 E-004
$d\bar{d} \rightarrow e^- e^+ gg$	1.3620189441 E-005	2.4684280244 E-004
$u\bar{u} \rightarrow e^- e^+ u\bar{u}$	6.9320177545 E-006	2.1474734072 E-004
$u\bar{u} \rightarrow e^- e^+ c\bar{c}$	1.8468108910 E-007	1.8007297663 E-006
$d\bar{d} \rightarrow e^- e^+ d\bar{d}$	1.0023268662 E-005	3.1647659850 E-004
$d\bar{d} \rightarrow e^- e^+ s\bar{s}$	2.3673784898 E-007	2.4179197657 E-006
$u\bar{u} \rightarrow e^- e^+ d\bar{d}$	6.6505600059 E-007	1.3323314116 E-006

Table 1. Partonic subprocesses and corresponding values for the Born squared amplitudes and the interference between the tree-level and the one-loop amplitudes. Momenta are given in eq. (A.1), whereas physical parameters are reported in the text. Processes that can be obtained by crossing are not reported.

the usual factor

$$c_\Gamma = \frac{(4\pi)^\epsilon}{\Gamma(1-\epsilon)}, \quad (\text{A.2})$$

are reported in Table 1, together with the corresponding partonic subprocesses and the Born squared amplitudes. The physical parameters chosen are as reported in section 3.1, but here the renormalization scale have been set equal to m_Z . The results for the virtual amplitudes are divided by $\alpha_s/2\pi$, *i.e.* they do not contain the extra power of the strong coupling constant. We stress that with the **BlackHat** version that has been used in this work these amplitudes are computed in the large m_t limit, and the axial contributions due to fermionic loops are not included. It has been explicitly checked that the above results agree with the same amplitudes obtained with **MCFM**, when the aforementioned contributions are turned off. Agreement between **BlackHat** and **MCFM** has been obtained also using $\hat{H}_T/2$ or the Z -boson transverse mass as renormalization scale.

References

- [1] Z. Bern, G. Diana, L. Dixon, F. Febres Cordero, S. Hoche, et al., *Driving Missing Data at Next-to-Leading Order*, *Phys.Rev.* **D84** (2011) 114002, [[arXiv:1106.1423](#)].
- [2] D. L. Rainwater, D. Zeppenfeld, and K. Hagiwara, *Searching for $H \rightarrow \text{tau tau}$ in weak boson fusion at the CERN LHC*, *Phys.Rev.* **D59** (1998) 014037, [[hep-ph/9808468](#)].
- [3] T. Plehn, D. L. Rainwater, and D. Zeppenfeld, *A Method for identifying $H \rightarrow \text{tau tau} \rightarrow e+-mu+-p(T)$ at the CERN LHC*, *Phys.Rev.* **D61** (2000) 093005, [[hep-ph/9911385](#)].
- [4] J. M. Campbell and R. K. Ellis, *Next-to-leading order corrections to $W^+ 2 \text{ jet}$ and $Z^+ 2 \text{ jet}$ production at hadron colliders*, *Phys.Rev.* **D65** (2002) 113007, [[hep-ph/0202176](#)].
- [5] J. M. Campbell, R. K. Ellis, and D. L. Rainwater, *Next-to-leading order QCD predictions for $W + 2 \text{ jet}$ and $Z + 2 \text{ jet}$ production at the CERN LHC*, *Phys.Rev.* **D68** (2003) 094021, [[hep-ph/0308195](#)].
- [6] C. Oleari and D. Zeppenfeld, *QCD corrections to electroweak $\nu(l) j j$ and $l+l-j j$ production*, *Phys.Rev.* **D69** (2004) 093004, [[hep-ph/0310156](#)].

- [7] S. Frixione and B. R. Webber, *Matching NLO QCD computations and parton shower simulations*, *JHEP* **06** (2002) 029, [[hep-ph/0204244](#)].
- [8] S. Frixione, P. Nason, and B. R. Webber, *Matching NLO QCD and parton showers in heavy flavour production*, *JHEP* **08** (2003) 007, [[hep-ph/0305252](#)].
- [9] P. Nason, *A new method for combining NLO QCD with shower Monte Carlo algorithms*, *JHEP* **11** (2004) 040, [[hep-ph/0409146](#)].
- [10] S. Frixione, P. Nason, and C. Oleari, *Matching NLO QCD computations with Parton Shower simulations: the POWHEG method*, *JHEP* **11** (2007) 070, [[arXiv:0709.2092](#)].
- [11] S. Alioli, P. Nason, C. Oleari, and E. Re, *Vector boson plus one jet production in POWHEG*, *JHEP* **01** (2011) 095, [[arXiv:1009.5594](#)].
- [12] S. Alioli, K. Hamilton, P. Nason, C. Oleari, and E. Re, *Jet pair production in POWHEG*, *JHEP* **04** (2011) 081, [[arXiv:1012.3380](#)].
- [13] A. Kardos, C. Papadopoulos, and Z. Trocsanyi, *Top quark pair production in association with a jet with NLO parton showering*, *Phys.Lett.* **B705** (2011) 76–81, [[arXiv:1101.2672](#)].
- [14] S. Alioli, S.-O. Moch, and P. Uwer, *Hadronic top-quark pair-production with one jet and parton showering*, *JHEP* **1201** (2012) 137, [[arXiv:1110.5251](#)].
- [15] L. D’Errico and P. Richardson, *Next-to-Leading-Order Monte Carlo Simulation of Diphoton Production in Hadronic Collisions*, *JHEP* **1202** (2012) 130, [[arXiv:1106.3939](#)].
- [16] S. Hoeche, F. Krauss, M. Schonherr, and F. Siegert, *A critical appraisal of NLO+PS matching methods*, [[arXiv:1111.1220](#)].
- [17] R. Frederix, S. Frixione, V. Hirschi, F. Maltoni, R. Pittau, et al., *aMC@NLO predictions for Wjj production at the Tevatron*, *JHEP* **1202** (2012) 048, [[arXiv:1110.5502](#)].
- [18] S. Hoeche, F. Krauss, M. Schonherr, and F. Siegert, *$W+n$ -jet predictions with MC@NLO in Sherpa*, [[arXiv:1201.5882](#)].
- [19] J. M. Campbell, R. K. Ellis, R. Frederix, P. Nason, C. Oleari, et al., *NLO Higgs boson production plus one and two jets using the POWHEG BOX, MadGraph4 and MCFM*, [[arXiv:1202.5475](#)].
- [20] S. Alioli, P. Nason, C. Oleari, and E. Re, *A general framework for implementing NLO calculations in shower Monte Carlo programs: the POWHEG BOX*, *JHEP* **06** (2010) 043, [[arXiv:1002.2581](#)].
- [21] K. Hagiwara and D. Zeppenfeld, *Helicity Amplitudes for Heavy Lepton Production in $e+e-$ Annihilation*, *Nucl.Phys.* **B274** (1986) 1.
- [22] K. Hagiwara and D. Zeppenfeld, *Amplitudes for Multiparton Processes Involving a Current at $e+e-$, $e+e-p$, and Hadron Colliders*, *Nucl.Phys.* **B313** (1989) 560.
- [23] J. Alwall et al., *MadGraph/MadEvent v4: The New Web Generation*, *JHEP* **09** (2007) 028, [[arXiv:0706.2334](#)].
- [24] Z. Bern, L. J. Dixon, and D. A. Kosower, *One loop amplitudes for $e+e-$ to four partons*, *Nucl.Phys.* **B513** (1998) 3–86, [[hep-ph/9708239](#)].
- [25] C. Berger, Z. Bern, L. Dixon, F. Febres Cordero, D. Forde, et al., *An Automated Implementation of On-Shell Methods for One-Loop Amplitudes*, *Phys.Rev.* **D78** (2008) 036003, [[arXiv:0803.4180](#)].

- [26] T. Binoth, F. Boudjema, G. Dissertori, A. Lazopoulos, A. Denner, et al., *A Proposal for a standard interface between Monte Carlo tools and one-loop programs*, *Comput.Phys.Commun.* **181** (2010) 1612–1622, [[arXiv:1001.1307](#)].
- [27] T. Gleisberg, S. Hoeche, F. Krauss, M. Schonherr, S. Schumann, et al., *Event generation with SHERPA 1.1*, *JHEP* **0902** (2009) 007, [[arXiv:0811.4622](#)].
- [28] F. Krauss, R. Kuhn, and G. Soff, *AMEGIC++ 1.0: A Matrix element generator in C++*, *JHEP* **0202** (2002) 044, [[hep-ph/0109036](#)].
- [29] J. Pumplin et al., *New generation of parton distributions with uncertainties from global QCD analysis*, *JHEP* **07** (2002) 012, [[hep-ph/0201195](#)].
- [30] M. Cacciari, G. P. Salam, and G. Soyez, *The Anti- $k(t)$ jet clustering algorithm*, *JHEP* **0804** (2008) 063, [[arXiv:0802.1189](#)].
- [31] M. Cacciari and G. P. Salam, *Dispelling the N^3 myth for the k_t jet-finder*, *Phys. Lett.* **B641** (2006) 57–61, [[hep-ph/0512210](#)].
- [32] M. Cacciari, G. P. Salam, and G. Soyez, *FastJet user manual*, [arXiv:1111.6097](#).
- [33] D. L. Rainwater, R. Szalapski, and D. Zeppenfeld, *Probing color singlet exchange in $Z + two jet$ events at the CERN LHC*, *Phys.Rev.* **D54** (1996) 6680–6689, [[hep-ph/9605444](#)].
- [34] P. Nason and C. Oleari, *NLO Higgs boson production via vector-boson fusion matched with shower in POWHEG*, *JHEP* **02** (2010) 037, [[arXiv:0911.5299](#)].
- [35] T. Plehn, D. L. Rainwater, and D. Zeppenfeld, *Determining the structure of Higgs couplings at the LHC*, *Phys.Rev.Lett.* **88** (2002) 051801, [[hep-ph/0105325](#)].
- [36] **ATLAS Collaboration** Collaboration, G. Aad et al., *Measurement of the production cross section for Z/γ^* in association with jets in pp collisions at $\sqrt{s} = 7$ TeV with the ATLAS detector*, *Phys.Rev.* **D85** (2012) 032009, [[arXiv:1111.2690](#)].
- [37] L. D’Errico and P. Richardson, *A Positive-Weight Next-to-Leading-Order Monte Carlo Simulation of Deep Inelastic Scattering and Higgs Boson Production via Vector Boson Fusion in Herwig++*, [arXiv:1106.2983](#).
- [38] S. Frixione, P. Nason, and G. Ridolfi, *A Positive-Weight Next-to-Leading-Order Monte Carlo for Heavy Flavour Hadroproduction*, *JHEP* **09** (2007) 126, [[arXiv:0707.3088](#)].
- [39] S. Alioli, K. Hamilton, and E. Re, *Practical improvements and merging of POWHEG simulations for vector boson production*, *JHEP* **1109** (2011) 104, [[arXiv:1108.0909](#)].